EVALUATION OF 3D PRINTED HELICAL GEARS WITH LATTICE STRUCTURE BY FINITE ELEMENT ANALYSIS

Magda Mihael, *Babeș-Bolyai University, Cluj-Napoca, ROMANIA*
Korka Zoltan-Iosif* (corresponding author), *Babeș-Bolyai University, Cluj-Napoca, ROMANIA*
Turiac Raul-Rusalin, *Babeș-Bolyai University, Cluj-Napoca, ROMANIA*

ABSTRACT: The contemporary state of Additive manufacturing (AM), through numerous, previous advancements, and refining of processes, has developed into a reliable and flexible 3D manufacturing technology, making significant advancements in mechanical component design. To that end, it has facilitated the fabrication of gears that incorporate internal lattice structures which, in contrast to gears derived from traditional manufacturing, offer and advantageous equilibrium between mass reduction and mechanical strength. Nonetheless, it is crucial to simulate the behavioral characteristics of these gears under operational loads, notably the distribution of stresses and strains, thereby validating design and preventing premature failure. Being mindful of this, Finite element analysis (FEA) allows us to precisely evaluate the effect of lattice structures on gear performance. This study presents a comprehensive process for modeling, simulating and interpreting results, thereby offering a practical framework for researchers and designers seeking to implement these solutions in real world applications.

KEY WORDS: additive manufacturing (AM), displacement, finite element analysis (FEA), lattice structures.

1. INTRODUCTION

Gears are fundamental power transmission components widely used across aerospace, automotive, marine, and industrial applications, where reliability and performance directly impact system efficiency [1]. The continuous demand for enhanced mechanical properties, reduced weight, and improved cost-effectiveness has driven innovations in both gear design and manufacturing methodologies. Traditional solid gear designs often carry significant material redundancy that limits their performance-to-weight ratio and increases overall system cost, particularly in weight-critical applications such as aircraft and high-speed machinery [2].

The emergence of additive manufacturing (AM) technology has revolutionized mechanical component design by enabling the fabrication of complex geometries that were previously impossible to achieve through conventional manufacturing processes [3]. This technological advancement has opened new possibilities for integrating lattice structures within gear bodies, a concept that combines the benefits of lightweight design with enhanced mechanical performance. Lattice structures are periodic cellular arrangements composed of interconnected struts that can be precisely tailored to achieve specific material properties while maintaining structural integrity [4]. These lattice structures, characterized by periodic cellular architectures, can be tailored to meet specific mechanical requirements while minimizing material consumption, a critical consideration in aerospace, automotive, and robotics applications where weight reduction directly impacts performance and energy efficiency [5]. When incorporated into gear systems, lattice structures can significantly reduce mass while preserving or even improving load-bearing capacity, which is particularly

advantageous for high-performance applications [6].

Finite Element Analysis (FEA) provides a powerful computational framework for evaluating the mechanical performance of these novel gear designs prior to physical prototyping. FEA enables detailed investigation of stress concentrations, deformation patterns, contact mechanics, and failure prediction under various loading scenarios, offering insights that are difficult or impossible to obtain through experimental testing alone [7], [8], [9]. Recent advances in computational modeling have demonstrated the effectiveness of FEA in predicting the behavior of additively manufactured components with complex internal architectures, validating its application to lattice-structured gears [10].

Despite growing interest in lightweight gear design, comprehensive studies evaluating the specific performance characteristics of 3D printed helical gears with lattice structures remain limited. Most existing research focuses either on solid 3D printed gears or on lattice structures in non-functional components, leaving a significant knowledge gap regarding the interaction between helical gear kinematics, contact stresses, and lattice structural mechanics. Furthermore, the influence of key design parameters—including lattice unit cell type (e.g., cubic, gyroid, diamond), relative density, orientation relative to loading direction, and material properties on gear performance requires systematic investigation.

This study addresses these gaps by conducting a comprehensive finite element analysis of 3D printed helical gears incorporating various lattice structures. The primary objectives are to: (1) evaluate the mechanical behavior and stress distribution patterns in lattice-structured helical gears under operational loading conditions; (2) compare the performance of different lattice topologies in terms of load-bearing capacity, weight reduction, and stress concentration factors; (3) assess the influence of lattice density and geometric parameters on gear strength and deformation; and (4) establish design guidelines for optimizing lattice-structured helical gears for specific applications. By integrating advanced computational modeling with additive manufacturing design principles, this research contributes to the development of next-generation lightweight power transmission systems with enhanced performance characteristics.

The findings of this investigation are expected to provide valuable insights for engineers and designers seeking to leverage additive manufacturing for gear production, particularly in weight-sensitive applications where traditional solid designs impose unacceptable mass penalties. Furthermore, the methodologies developed herein establish a framework for the virtual evaluation and optimization of complex lattice-structured mechanical components, accelerating the translation of AM design innovations from concept to practical implementation.

2. MATERIALS AND METHODS

The variant 0 (V0), presented in figure 1, is a base helical gear with 100% infill, selected for the application of lattice infills.

Figure 1. Dimetric view of variant V0 with 100% infill.

The base gear has the geometric parameters presented in table 1, while the lattice structures were designed in four distinctive variants (V1-V4).

Table 1. Base helical gear parameters.

Parameters	Symbol [m.u.]	Value
Gear module	m_n [mm]	2
Teeth number	z	75
Gear width	b [mm]	17
Helix angle	β [°]	10
Pressure angle	α [°]	20
Profile shift coefficient	x	-0.659
Tip diameter	d_a [mm]	153.496
Reference diameter	d [mm]	152.314
Root diameter	d_f [mm]	144.078
Gear Hub diameter	d_h [mm]	45
Gear rim diameter	d_r [mm]	130
Material	C45-EN 10083-2	

Each lattice pattern was manually sketched and applied to the zone between the hub and the gear rim, applying modifications specifically on the region between diameters Ø45mm and Ø130mm, as shown in figure 2. The material initially present at the infill zone was removed by an extruded cut command, for the exception of variant 4, where a cell cut seed was used instead.

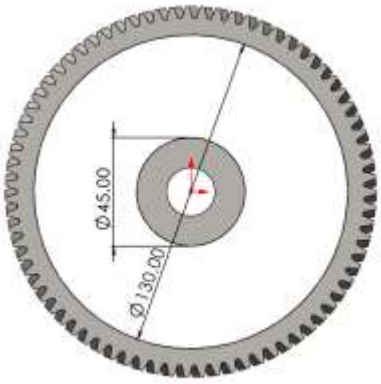

Figure 2. Front view of infill zone.

Variants V1 to V4 had their lattice patterns created with 3 different rib thicknesses: 0.8mm, 1.2mm and 1.6mm, where their combined impact on the gears mass is shown in table 2.

Table 2. Rib thickness impact on gear mass.

Mass [g]			
Variant code	Rib thickness [mm]		
	0.8	1.2	1.6
V0	2266.44		
V1	1041.91	1204.23	1366.56
V2	1380.15	1632.99	1835.47
V3	1306.42	1540	1741.15
V4	1301.65	1478.32	1605.01

A visual representation of the rib thickness influence on gear masses is shown for all the investigated variants in figure 3.

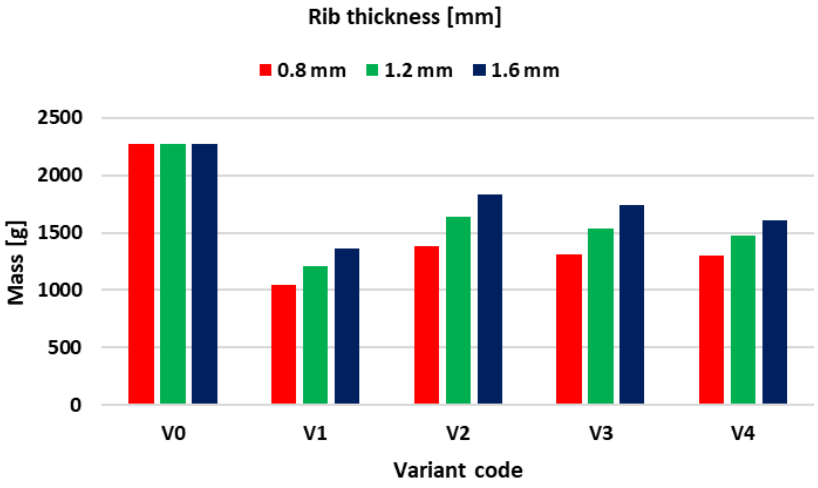

Figure 3. Rib thickness impact on gear mass.

Variant 1 (V1- with linear pattern infill), as shown in figure 4, was realized by sketching two lines, parallel to a reference axis on both sides, followed by determining the distance from the axis (0.4mm, 0.6mm, 0.8mm) corresponding to each rib thickness (0.8mm, 1.2mm, 1.6mm), extruding the sketch and applying a circular pattern at a 360° total angle, consisting of 72 instances. This variant has a rudimentary lattice design and was intended to serve as a comparison with the other, more complex, lattice patterns.

Figure 4. Dimetric view of V1 pattern infill.

Variant 2 (V2- circular arc infill), as shown in figure 5, was accomplished by sketching one circular arc with a radius of 60 mm. The arc has been rotated around the starting point on the hub, so that the line joining that point to the center of the arc forms a 45° angle with the vertical axis of the gear.

Figure 5. Dimetric view of V2 pattern infill.

An offset command followed to define the rib thickness (0.8mm, 1.2mm, 1.6mm) and, by using the mirror command, the rib was multiplied on the opposite side of the vertical axis of the gear. Finaly, the sketch was extruded and a circular pattern at a 360° total angle, consisting of 72 instances, was applied. Variant 3 (V3- 45° linear pattern infill) as shown in figure 6, was designed similarly to V2. The difference from the previous version was that the curved shape of the ribs was replaced by a linear one.

Figure 6. Dimetric view of V3 pattern infill.

Variant 4 (V4- honeycomb pattern infill) is shown in figure 7. Compared to the previously described variants, V4 diverges in its realization, as no initial profile sketch was used and the infill was initially left at 100%.

Figure 7. Dimetric view of V4 pattern infill.

In turn, a fill pattern feature was utilized, with the boundary zone located between the hub and the rim. A vertical axis was sketched followed by a reference line inclined at 45° to the axis. This line was used as the pattern direction guide. Instead of selecting extruded

features for multiplication, a hexagonal cell cut seed was chosen, with an inner radius of 1.5 mm and a corresponding outer radius of 1.7 mm. The stagger angle was fixed at 30°, while the spacing between the cells was set to 3.8mm, 4.2mm, 4.6mm, corresponding to each rib thickness (0.8mm, 1.2mm, 1.6mm).
While these infill variants (V1-V4) show considerable mass variation in relation to the base model (V0), as presented in table 3, we intended to find out how these lattice structures affect the gear rigidity.

Table 3. Mass variation compared to V0.

Mass variation [%]			
Variant code	Rib thickness [mm]		
	0.8	1.2	1.6
V0	0%		
V1	-58.03%	-46.87%	-39.71%
V2	-39.11%	-27.95%	-19.02%
V3	-42.36%	-32.05%	-23.18%
V4	-42.57%	3-4.77%	-29.18%

Utilizing the Finite element analysis (FEA) feature available in SolidWorks, studies on static load were applied, as shown in figure 8. The purpose was to find a favourable balance between gear mass and rigidity.

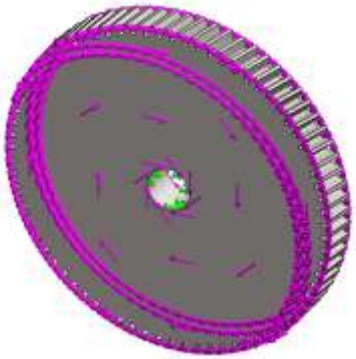

Figure 8. Fixture condition and load applied in the static analysis.

Details of the lattice structure designs (V1-V4), with the gradual increase in rib thickness, are shown in figure 9.

V1- 0.8

V1- 1.2

V1- 1.6

V2- 0.8

V2- 1.2

V2- 1.6

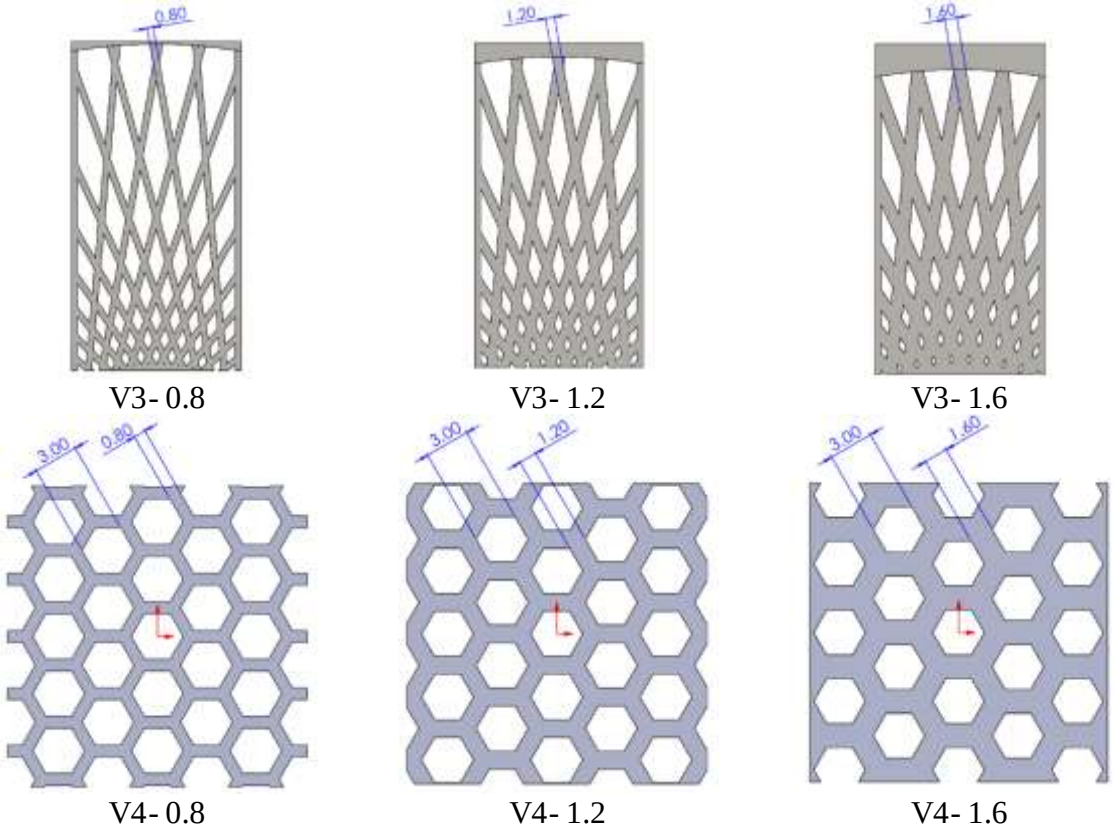

Figure 9. Lattice structure design (V1-V4).

The static load analysis for the five geometries was conducted by setting an axis constraint on the inner diameter of the gear and applying a total torque of 1000 Nm on the gear rim, on both sides.

3. RESULTS

The obtained stress results are shown in table 4, while figure 10 presents a visual representation of the behaviors displayed by the gear variants in relation to the rib thicknesses.

Table 4. Von Mises stress results.

Maximum stress [MPa]			
Variant code	Rib thickness [mm]		
	0.8	1.2	1.6
V0	155.75		
V1	2698.34	1167.35	677.27
V2	149.97	154.9	156.55
V3	154.73	151.86	153.42
V4	808.35	209.44	168.56

Variant V1 shows very high stress values which are far exceeding the material yield strength (580 MPa). While these values drop considerably with each gradual rib thickness increase, the presence of a greater volume of mass that takes on the torsional stress is not enough to bring the stress under the elasticity limit.

Variants V2 and V3 show variable stress values which are much closer to the results obtained for the base helical gear (V0). This can be explained by the increased rib thickness, as overlaps lead to smaller gaps at the hub of the gear, thereby resulting in variable stress values specific to each unique infill lattice and thickness utilized.

Variant V4 also indicates high stress values, considerably over the material yield strength at a rib thickness of 0.8 mm. These stress values drop drastically, as the rib thickness is increased to 1.2 and 1.6 mm respectively. This can be explained by the presence of a higher volume of material that opposes the torsional load.

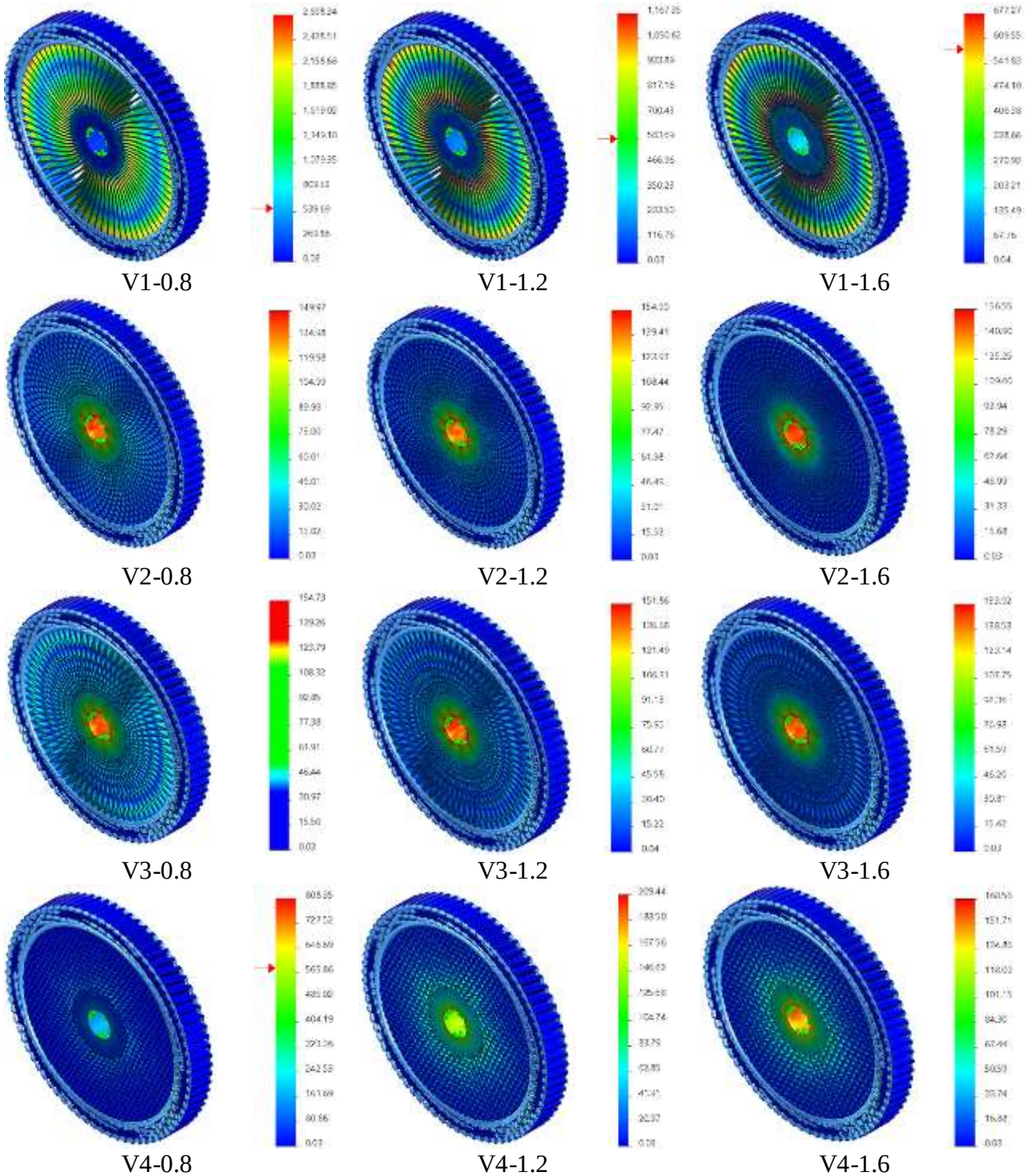

Figure 10. Von Mises stress results [MPa].

Table 5 presents the displacement results obtained from the static study. The data demonstrates a consistent pattern: as rib thickness increases, displacement values decrease. Figure 11 provides a. visual representation of these trends.

Table 5. Resultant displacement results.

Maximum displacement [mm]			
Variant code	Rib thickness [mm]		
	0.8	1.2	1.6
V0	0.041		
V1	17.312	5.533	2.446
V2	0.057	0.05	0.046
V3	0.081	0.063	0.054
V4	0.101	0.071	0.061

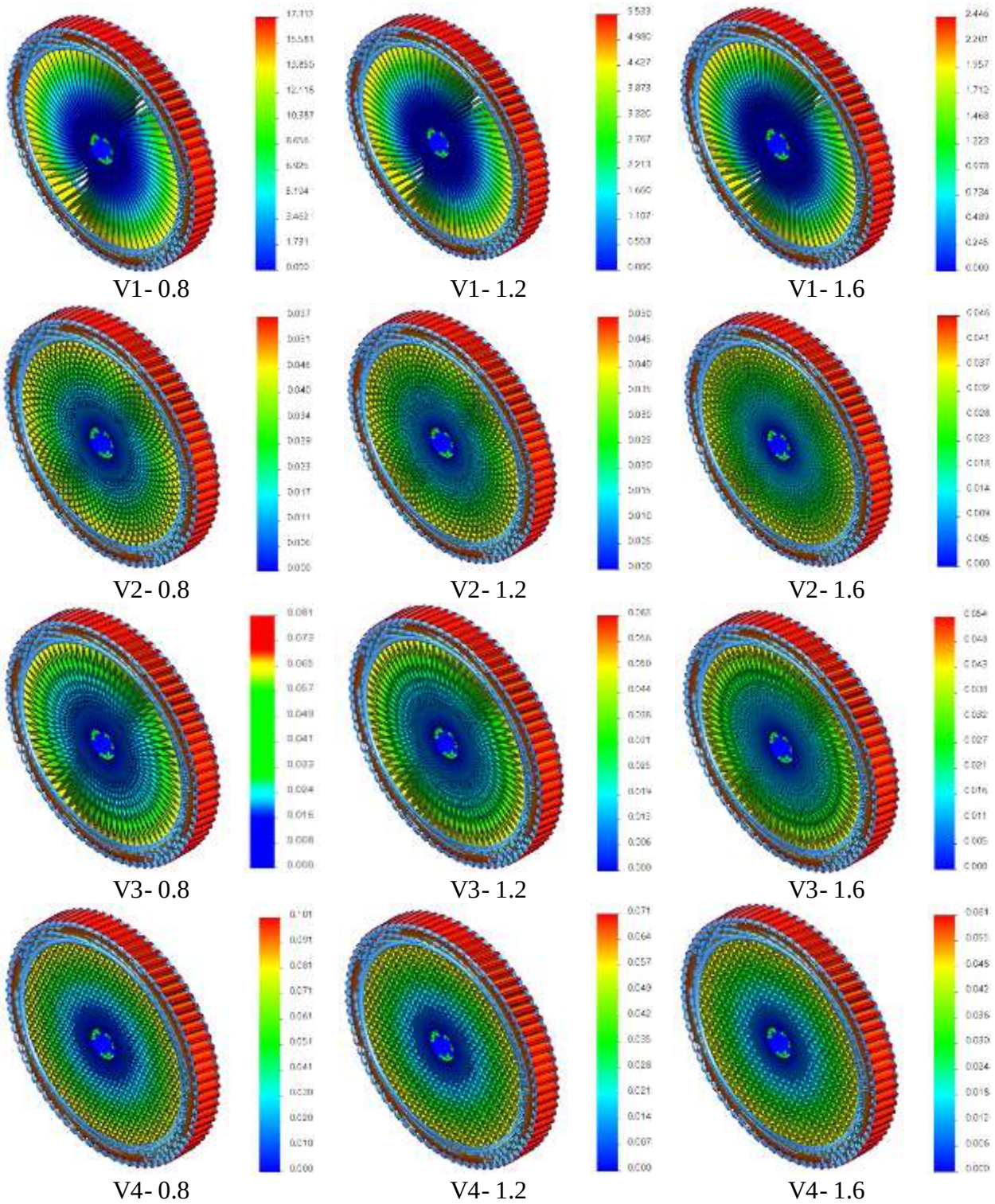

Figure 11. Displacement results [mm].

Observing figure 10 and table 4, one can deduce that V1 and V4 clearly benefit from the increased rib thickness, as the lowest von Mises stress values are obtained at 1.6 mm. However, variants V2 and V3 present minor stress variations by increasing the rib thickness. While for V2, a slight drop in stress manifests at 1.2mm and increases again at 1.6mm, higher than the initial 0.8mm value, for V3, it is the opposite. While a slight increase is obtained at 1.2mm, it drops at 1.6mm, displaying an almost equal value as for the initial 0.8mm rib thickness. This phenomenon is corelated to fluctuating gaps at the hub of the gear, thereby resulting in

variable stress values specific to each unique infill lattice and thickness utilized.

Regarding the maximum resultant displacements, the simulations performed clearly demonstrate that by increasing the rib thicknesses, lower displacements are obtained. The most sensitive variants are again V1 and V4, while at V2, by doubling the rib thickness, a 19.3% smaller displacement is obtained.

The results obtained by simulation imply divergent behavior, based on the lattice used as well as the thickness utilized.

4. CONCLUSIONS

The study aimed to determine the performance of gears with variable lattice infills under static torque loads, and corroborating the results to mass reduction.

The results are diverse, as many parameters that affect the study results are interconnected and some disadvantages must be accepted.

For variants V1 and V4 an equilibrium was achieved at a rib thickness of 1.6mm with a mass reduction of 39.71% for V1 and 29.18% for V4 respectively. For variant V2 an acceptable balance was achieved at a rib thickness of 0.8mm, with the corresponding mass reduction of 39.11%. For variant V3 an acceptable equilibrium was achieved at a rib thickness of 1.2mm, with the corresponding reduction in mass of 32.05%.

The very high stress values obtained for variant V1 are due to its simplistic infill design as well as the constraints of this study. It proves that more advanced lattice bodies better oppose torque loads.

As the study shows, there is no fixed advantage between mass reduction and gear performance, thereby indicating that each lattice type must be fine-tuned and customized to fit specific loads.

Ultimately, the study adds findings to existing literature with the purpose of helping designers to optimize gear lattice structures.

REFERENCES

[1] Mech, P. I., Sugunesh, E. A., and Mertens, A. J. A comprehensive study on Hertzian contact stress behaviour of engineering thermoplastic gears using 3D finite element analysis, Engineering Science, May 2023.

[2] Ilinc, C., Ramadan, I. N., Neaca, A., Petrescu, M. G., and Laudacescu, E. Finite Element Analysis of 3D-Printed Gears: Evaluating Mechanical Behaviour Through Numerical Modelling, Materials, Sep. 2025.

[3] Li, Y., Jiang, D., Zhao, R., Wang, X., Wang, L., and Zhang, L. High Mechanical Performance of Lattice Structures Fabricated by Additive Manufacturing, Metals, Oct. 2024.

[4] Zhou, Q., Xing, X., Gong, X., Zhou, Z., Zhang, X., and Hu, X. Enhanced compressive mechanical properties of different topological lattice structures fabricated by additive manufacturing, Mechanics of Advanced Materials and Structures, Jul. 2024.

[5] Omar, W. K., and Hamid, A. A. Enhancement over Conventional 3D Printed Lattice Structures and Investigation of their Mechanical Properties Using FEM Modeling and Experimental Studies, Advanced Journal of Chemistry, Jun. 2025.

[6] Kofolu, M., Yunus, D., and Ercan, N. Lattice optimization of fiber-reinforced polymer parts fabricated by additive manufacturing: the impact of Bezier curve order on mechanical properties, Rapid Prototyping Journal, May 2024.

[7] Ilincă, C. N., Ramadan, I. N., Neacșa, A., Petrescu, M. G., Laudacescu, E. V. Finite Element Analysis of 3D-Printed Gears: Evaluating Mechanical Behaviour Through Numerical Modelling, PubMed, Sep. 2025.

[8] Korka, Z. I., Cojocaru, V., Miclosina C. O. Influence of the Mesh parameters on Stresses and Strains in FEM Analysis of a Gear Housing, ResearchGate, Oct. 2013.

[9] Korka, Z. I., Cojocaru, V., Miclosina C. O. Modal - Based Design Optimization of a Gearbox Housing, Romanian Journal of Acoustics and Vibration, Sep, 2019.

[10] Ramadani, R., Pal, S., Belšak, A., Predan, J. Selective Laser Melting of a Ti-6Al-4V Lattice-Structure Gear: Design, Topology Optimization, and Experimental Validation, Applied Sciences, Jul. 2025.